

Received November 9, 2020, accepted November 15, 2020, date of publication November 18, 2020, date of current version December 7, 2020.

Digital Object Identifier 10.1109/ACCESS.2020.3039055

# Mechanical Condition Identification and Prediction of Spring Operating Mechanism of High Voltage Circuit Breaker

YAKUI LIU<sup>1</sup>, GUOGANG ZHANG<sup>1</sup>, (Member, IEEE), CHENCHEN ZHAO<sup>1</sup>, SHENG LEI<sup>1</sup>, HAO QIN<sup>1</sup>, AND JINGGANG YANG<sup>2</sup>, (Member, IEEE)

<sup>1</sup>State Key Laboratory of Electrical Insulation and Power Equipment, Xi'an Jiaotong University, Xi'an 710049, China

<sup>2</sup>Jiangsu Electric Power Company Research Institute, State Grid Corporation of China, Nanjing 211103, China

Corresponding author: Guogang Zhang (ggzhang@mail.xjtu.edu.cn)

This work was supported by the State Grid Corporation of China (SGCC) "Research on Key Technologies of Mechanical Condition Assessment and Fault Diagnosis for High Voltage Switchgear".

**ABSTRACT** Spring operation mechanism is widely used in high voltage circuit breakers, and its reliability is related to the ability of the circuit breaker breaking fault current. During the life cycle of spring operating mechanism, stress relaxation, metal fatigue, and any other mechanical defects are easily occurring. And the mechanical performance of the circuit breaker will be influenced by the above defects. Therefore, identifying and predicting the mechanical conditions of the spring operation mechanism can improve the reliability of the circuit breaker. In the present paper, the 252 kV circuit breakers are used as test objects. Firstly, the spring stress relaxation test, the life-cycle test, and the failure simulated test of 252 kV circuit breakers are carried out. Secondly, a multi-body dynamics simulation model of the experimental prototype is established. Thirdly, support vector machine, random forest, and deep neural network are used in the condition identification of the circuit breaker to compare their performances. Then, the prediction model of spring in stress relaxation test is built, however, the model is not suitable for the life-cycle test of repeat close-open operation. Finally, the remaining useful life prediction model is proposed by using Wiener Process.

**INDEX TERMS** Spring operation mechanism, circuit breaker, random forest, Wiener process.

## I. INTRODUCTION

High voltage circuit breakers with spring operating mechanisms are widely used in the power grid. The mechanical condition of the breaker is related to whether it can interrupt fault current, which is important for the protection in the power system. Consequently, the mechanical condition identification of circuit breaker has become a hot topic for many years.

### A. PREVIOUS WORK

#### 1) FAULT DIAGNOSE OF CIRCUIT BREAKER

In the diagnose of the circuit breaker, contact displacement [1], electromagnet coil current [2], and vibration characteristics [3]–[5] are widely used as diagnosis parameters.

Contact displacement could effectively reveal the condition of the operating mechanism. Ali Asghar Razi-Kazemi *et al.* hold the view that any changes in time or speed is most likely an indication of a damaged spring, over travel is an indication

The associate editor coordinating the review of this manuscript and approving it for publication was Lei Shu<sup>1</sup>.

of a failure in damper, and any changes in rising time of contact displacement is most likely caused by a failure in coils of the operating mechanism [6].

The closing and opening electromagnet irons play important and critical roles in the operating mechanism, and the movement process of the iron core could be described by the coil current [7]. Then, the signals can be extracted based on a deep belief network [8], a real-time diagnosis algorithm [9], or a fuzzy-probabilistic-based condition assessment algorithm [10] to assess the CB operation performance. The algorithms are adopted to assist in the construction of a high-quality fault diagnosis model.

The vibration signal has the characteristics of highly non-linear, non-stationary, and corrupted by heavy garbage noise, which makes it very difficult to precisely extract effective features for machinery fault diagnosis. To address this issue, many methods have been proposed. For example, an energy entropy of Hilbert marginal spectrum based on vibrational mode decomposition is presented to analyze it [11]; another research introduced a non-linear feature mapping in the wavelet package time-frequency energy rate feature space

based on random forest binary coding to extend the feature width [12]. In addition, two layers of independent one-class support vector machines are adopted to distinguish normal or fault conditions with known or unknown fault types respectively. On this basis, a support vector machine is used to recognize the specific fault type [13].

Besides, more and more multi-parameters (including contact displacement, current, and vibration) monitoring systems were proposed [3]. Fatemeh Nasri Rudsari *et al.* diagnosed the faults based on coil current and contact displacement through a modified support vector machine [14].

## 2) FAILURE ANALYSIS OF SPRING MECHANISM

The mechanism components endure hundreds of repeated stress owing to the repetitiveness of close-open operation. As a result, some parts and components are prone to fail during cycling repeated stress. For the 35kV-252kV high voltage circuit breaker, the spring mechanism is one of the most common operating mechanisms.

According to the international surveys on circuit-breaker reliability, the failure of the operating mechanism is much higher than other subassemblies in breakers [15]. Consequently, fatigue failure of circuit breaker energy storage spring has drawn a series of attentions [16], [17]. Surface decarburization has been proved to influence the service performance of spring steel directly. The decarburized layer was significantly modified by turning into a strengthened layer with gradient microstructure after surface spinning strengthening treatment, which effectively extended the bending fatigue life of spring steel [18]. Darko *et al.* proposed that the continuous contact between the coils formed corrosion pits that served as crack initiation points leading to the final fracture [19]. In another paper, a high-speed camera has been used to capture the deformation of the operating mechanism spring [20].

The reliability of circuit breakers is critical to ensure the safe operation of the power system. In order to investigate the reliability of high voltage SF<sub>6</sub> circuit breakers, a statistical approach is applied, which can estimate the remaining lifetime and the failure rate of circuit breakers based on the failure data [21]. T.M. Lindquist *et al.* proposed the use of the conditional failure intensity to quantify the effect of maintenance for breakers [22]. In the maintenance plan of circuit breakers, the effects of the failures on the cost of the expected unused energy should be considered [23].

## B. CONTRIBUTIONS

The primary contributions of our study can be summarized as follows:

1) The stress relaxation and fatigue tests are carried out to compare the influences on the mechanical performances of the circuit breaker. At present, there is no research on the mechanical life prediction of the spring operating mechanism of the high-voltage circuit breaker, and there is no corresponding mathematical model. In the present paper, to obtain the mechanical characteristic curves of the circuit breaker

under normal and spring fatigue conditions, the fatigue life test is carried out. The spring operating mechanism is expensive and is not suitable for large sample tests, so the RUL model can only depend on the degradation data of a single sample. Based on the degradation data of the spring mechanism that is obtained from the fatigue life test, the RUL model of the spring operating mechanism based on the Wiener process is established.

2) In the traditional failure simulation method of spring operating mechanism, the normal state does not contain the aging and wear of the spring operating mechanism, and the adjusting of the spring compression is used to simulate the fatigue failure. However, there is a difference between the above simulated methods and the real conditions of the spring operating mechanism on the mechanical properties. Therefore, in the present paper, the normal state is randomly selected from the life-cycle test which contains the aging and wear of the spring operating mechanism, and a fatigued spring is used to simulated the fatigue failure.

3) For the diagnosis of the spring operation mechanism, not any researches aimed at using the random forest algorithm to realize high-voltage circuit breaker fault diagnosis through contact displacement signals. Compared with the vibration and coil current, the installation method of the contact displacement sensor has less influence on the circuit breaker, and the displacement signal is more repeatability. Therefore, the contact displacement is used to construct the feature matrix. Then, the performances of SVM, RF, and DNN in the condition identifying of the circuit breaker are compared.

## C. WORK ORGANIZATION

The remainder of the presented paper is organized as follows: Section II introduces the stress relaxation test of the spring, the fault simulation test, and the life-cycle circuit breaker tests. In section III, a dynamic simulation model of the circuit breaker is built. Then, SVM, RF, and DNN are used to identify the failures in section IV. Finally, the life prediction model of the spring operation mechanism is established.

## II. EXPERIMENTS

According to previous studies, the failure of spring was simulated by adjusting the compression of closing and opening spring. The above method is easy to implement, but the fatigue failure is caused by the decrease of stiffness rather than the change of compression. Therefore, the fatigue spring will be installed in the present paper.

Two LW30-252 breakers with spring operating mechanism are used, and the mechanical parameters can be seen in TABLE 1. The average closing and opening speed is defined as the speed of 80% of the travel of the moving contact in the middle, while removing both 10% of the front and back of the total travel of the moving contact. Breaker I is used to simulating the faults, and breaker II is used to carry the mechanical life-cycle test of closing and opening spring. The experiments are shown as follows.

**TABLE 1.** The parameters of the test circuit breakers.

| Parameter             | Value   | Unit |
|-----------------------|---------|------|
| Average closing speed | 4.4±0.6 | m/s  |
| Average opening speed | 8.4±0.6 | m/s  |
| Closing time          | 90±15   | ms   |
| Opening time          | 30±7    | ms   |

**A. STRESS RELAXATION TEST**

Stress relaxation occurs in the energy storage stage of the spring. According to the mechanical mechanism of the circuit breaker, the closing force is provided by both closing and opening spring, and the opening force is only provided by opening spring.

To study the stress relaxation mechanism, the stress relaxation test of the spring is carried out. Firstly, the free height of the compression coil spring is defined as  $H_0$ , when the initial load  $P_0$  is added, the height of the spring is changed to  $H$ . Then, the height of the coil spring is fixed to  $H$  by bolts and nuts. After that, the spring is taken out from the fixing condition, and the load  $P_t$  when the height reaches  $H$  is measured. The above operation is repeated every certain time, and the load value of  $P_t$  in each test is recorded.

The tests have been carried out for 36 months with the same kind of spring, which is made of 60Si2CrVA. The spring experienced the hot-winding process, the high-pressure treatment, and the electrophoretic paint in the production.

In simple tension experiments, the relationship between strain and stress of spring submits Hook’s law within the limit of proportionality, and the law can be described as,

$$F = k \cdot (H - H_0) \tag{1}$$

where  $F$  is the spring force,  $k$  is the stiffness coefficient.

The relationship between stress and time in the test can be seen in FIGURE. 1. The results mean that the stiffness coefficient of the spring will drop quickly in the first 6 months (which can be seen in Stage I), then the downward trend slowed down (which can be seen in Stage II).

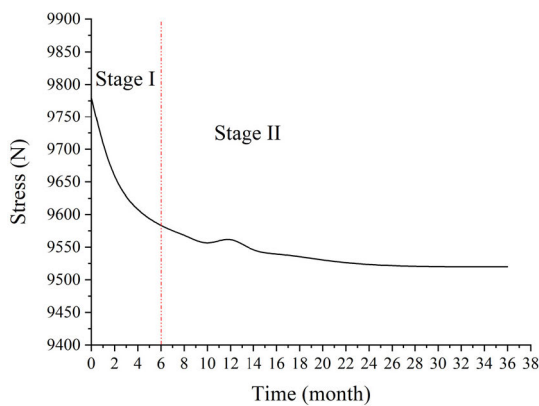


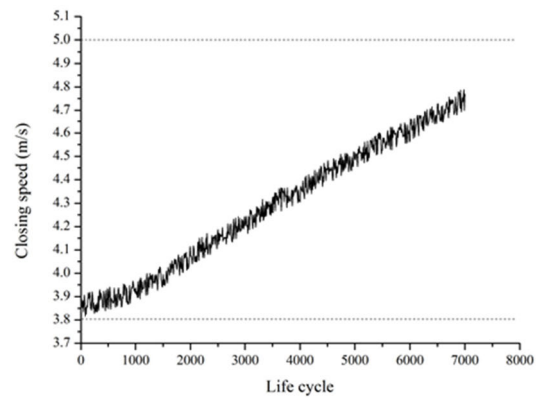
**FIGURE 1.** The relationship between stress and time in the stress relaxation.

**B. LIFE-CYCLE TEST**

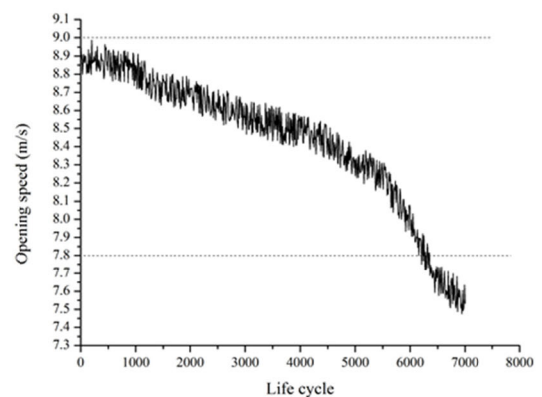
Metal fatigue of the spring occurs after multiple breaking actions. Therefore, the life-cycle test is carried out to simulate

metal fatigue defects. Due to the trend in the stress relaxation test, the life-cycle test is carried out in 6 months after the circuit breaker had been installed. In the life-cycle test, the circuit breaker experiences 7,000 breaking times without current carried, and the contact displacement has been measured concurrently.

The opening speed of movable contact is an important parameter for the circuit breaker, as soon as the contact speeds of breaker II in the life-cycle test are not meeting the required values of average speed in TABLE 1, then the mechanical life is regarded as the end. During the life-cycle test, the closing, and opening speed are calculated, which can be seen in FIGURE.2. The dots curve is the minimum required value of opening speed, the stability and the breaking capacity will be extremely harmed if the speed lower than the dots curve.



**a Closing speed versus life cycle**



**b Opening speed versus life cycle**

**FIGURE 2.** The speed curves in life-cycle test.

The results from the life-cycle test show that with the increase of life cycles, the opening speed decrease, while, the closing speed increase in turn. More specifically, the closing speed always within the normal range, but the opening speed is lower than the rated value at 6,000 times, which means that the breaker I can’t meet the mechanical requirements, and the spring can be considered as fatigue.

**C. SIMULATED FAILURE TEST**

**1) FATIGUE FAILURE**

The spring used in breaker II has endured thousands of impact, then it is removed and installed on breaker I to simulate the failure.

**2) LEAK OF OIL BUFFER FAILURE**

The oil buffer, as the name suggests, it acts as a buffer during the action of the circuit breaker. The purpose of the experiment is to simulate the failure caused by the aging and failure of oil buffer. Under the long-term operations, the oil will volatilize and leak. Therefore, the oil is pumped from the oil buffer in the experiment for simulating the fault.

**3) COMPOUND FAILURES**

Based on the single failure which has been simulated in the experiments, then multiple failures are discussed in the paper by combing with the single failures to form the compound failures.

**4) SUMMARY OF THE STATES**

Following the above methods, the states of the breaker considered in the present paper can be seen in Table 2, and the contact displacement curves can be seen in FIGURE.3. The normal condition is randomly selected from 1 to 1,000 times in the life-cycle test.

**TABLE 2. Summary of the states considered in this study.**

| Description of states                                | Category label | Sample number for training |
|--|----------------|----------------------------|
| Normal state   | Class 1        | 200                        |
| Closing spring fatigue                               | Class 2        | 50                         |
| Opening spring fatigue                               | Class 3        | 50                         |
| Leak of oil buffer                                   | Class 4        | 50                         |
| Both closing and opening spring fatigue              | Class 5        | 50                         |
| Closing spring fatigue as well as leak of oil buffer | Class 6        | 50                         |

The relationship between speed and spring force can be described as,

$$\frac{dv_o}{dt} = \frac{1}{M} (F_o + W_g - F_r - F_b - F_f) \quad (2)$$

$$\frac{dv_c}{dt} = \frac{1}{M} (F_c - W_g - F_r - F_b - F_f - F_o) \quad (3)$$

where  $v_o$  is the opening speed,  $v_c$  is the closing speed,  $M$  is equivalent motion mass,  $F_o$  is the opening spring force,  $F_c$  is the closing spring force,  $W_g$  is the gravity force,  $F_r$  is the reaction force of arc extinguishing chamber,  $F_b$  is the buffer force,  $F_f$  is the friction force.

In Class 2, the decrease of closing force decrease the closing speed, which is caused by fatigue of the closing spring; in Class 3, the fatigue of opening spring decrease the opening spring force, thus increase the closing speed; in Class 4, the leak of oil buffer decrease the buffer force, and increase the closing speed; in Class 5, both the opening and closing spring force decrease; in Class 6, the fatigue of

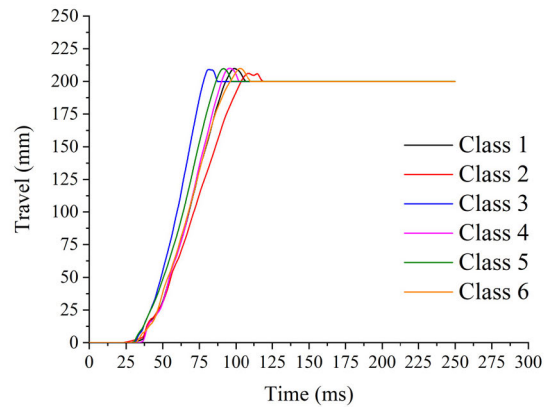


**FIGURE 3. The travel versus time under different conditions.**

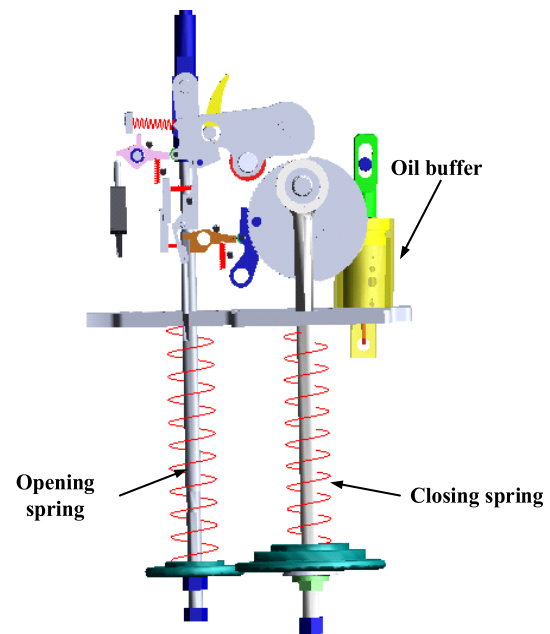


**FIGURE 4. Dynamic simulation model of circuit breaker by ADAMS.**

closing spring decrease the closing spring force, the leak of oil buffer decrease the buffer force at the same time.

**III. DYNAMIC SIMULATION MODEL BY ADAMS**

**A. THE ESTABLISHING METHOD OF DYNAMIC MODEL**

In this section, a three-dimensional model of the high-voltage circuit breaker is built. Then, the model is imported into ADAMS, a multi-body dynamic analysis software. Some constraints are added to the model, such as fixed pair, rotating pair, and sliding pair. Meanwhile, the stiffness coefficient and the damping coefficient are added to the spring, and the contact force parameters are set to components that may be contacted.

The simulation model can be seen in FIGURE.4, and the parameters of the spring which are used in the simulation can be seen in TABLE 3. After the simulation, the contact displacement of the normal condition can be seen in FIGURE.5.

TABLE 3. The parameters of the spring.

| Parameters                   | Closing spring | Opening spring |
|------------------------------|----------------|----------------|
| Material                     | 60Si2CrVA      | 60Si2CrVA      |
| Initial height (mm)          | 615            | 592            |
| Stiffness coefficient (N/mm) | 204.96         | 155.79         |
| Height at closing point (mm) | 471            | 344            |
| Height at opening point (mm) | 373            | 464            |

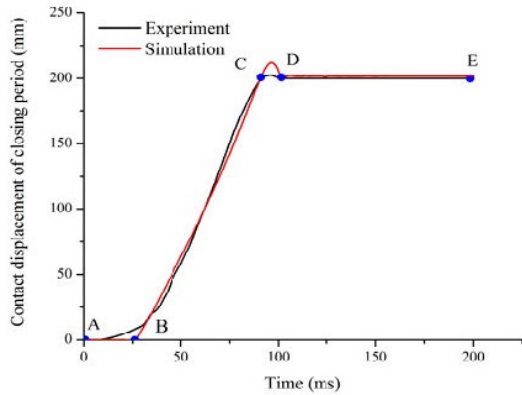


FIGURE 5. Comparison between simulation and experiment of closing period.

B. SPRING FATIGUE SIMULATION

It can be obtained from the fault simulation that the failure of the spring will influence the mechanical performance of the high voltage circuit breaker. According to the principle of the spring operating mechanism of the high-voltage circuit breaker, the mechanical characteristics in the closing period are affected by the opening spring and the closing spring. However, the mechanical characteristics in the opening period are only affected by the opening spring. When the opening spring is fatigued, its stiffness coefficient declines, and the pre-pressure reduces, resulting in a decrease in the opening speed.

During the life-cycle test of repeat close-open operation, the stiffness of the spring is hard to measure. However, based on the above (2) and (3), the coefficient can be calculated and verified by the multi-body dynamics simulation. In the simulation, the values of  $W_g, F_r, F_b, F_f$  are considered as constants, and the results are shown in FIGURE.6.

IV. CONDITION IDENTIFICATION OF CIRCUIT BREAKER

The operating mechanism including closing and opening spring, oil buffer, insulated tension pole, transmission mechanism, and many other machine parts. If one of them fails, the mechanical condition may be harmed. Therefore, identifying the hidden defects in advance will help to improve the reliability of the circuit breaker.

Many machine learning classifiers have been proposed in the diagnosis of the breaker, such as the support vector machine, depth learning network, and so on. Recently, Random Forest is adopted in the condition identifying due

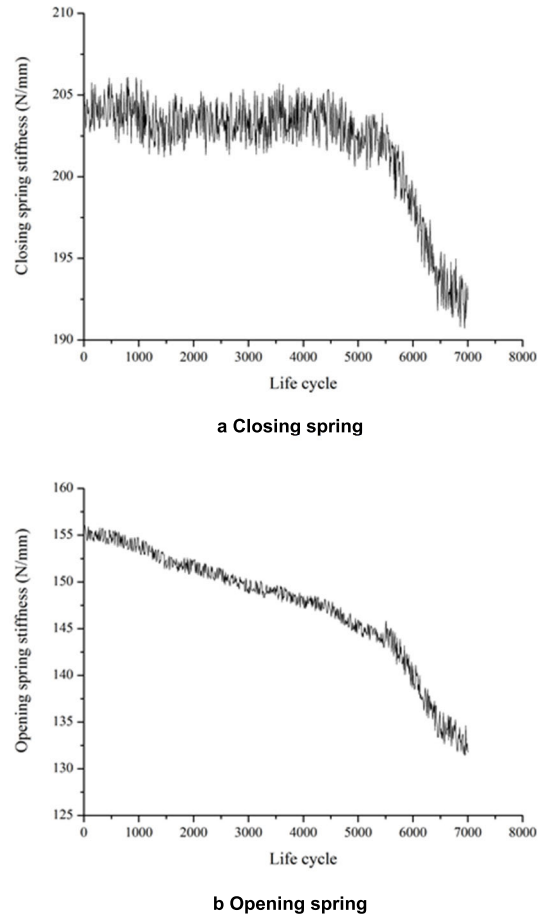


FIGURE 6. The relationship between spring stiffness and life cycle under life-cycle test.

to its great efficiency. However, there is no research on the comparison of the above methods in the mechanical condition identifying of the circuit breaker with the contact displacement. Therefore, support vector machine (SVM), random forest (RF), and deep neural network (DNN) are used in the condition identification of the circuit breaker to compare their performances. In the machine learning performance evaluation, confusion matrix, precision, recall rate, and F-measure are commonly used to describe the accuracy of the identification.

The precision, recall rate, and F-measure can be described as [24],

$$Precision = \frac{TP}{TP + FP} \tag{4}$$

$$Recall = \frac{TP}{TP + FN} \tag{5}$$

$$F\text{-measure} = \frac{2TP}{2TP + FP + FN} \tag{6}$$

where  $TP$  is the number of true positives,  $FP$  is the number of false positives, and  $FN$  is the number of false negatives.

For the circuit breaker, the states and samples are shown in Table 2. 450 sets of data are selected to train the model.

Meanwhile, the same conditions are simulated on another circuit breaker, and 225 sets of data are used to verify the correctness and efficiency of the algorithms.

**A. CONDITION IDENTIFICATION BY SVM**

SVM is a binary classification model. Its basic model is the linear classifier with the largest interval defined in the feature space. However, with the help of kernel function, SVM can be used as a nonlinear classifier. To improve the classification accuracy, the radial basis kernel function is selected as the kernel function. Then, the optimal values of the penalty factor ( $C = 100$ ) and the parameter of the radial basis kernel function ( $\gamma = 0.01$ ) are obtained by the 4-fold cross-validation grid search method.

It can be seen from Fig. 3 that the various curves have no difference before 25ms and after 125ms, so only the 25~125ms part is considered. The contact displacement of every 0.1ms is considered as one of the features. Besides, closing time, closing speed, and average speed together constitute the feature matrix. Therefore, the number of features is 1003.

The diagnosis results of SVM can be seen in FIGURE.7. Based on the confusion matrix, 5 sets of the testing data are not correctly identified. The precision, recall rate, and F-measure for different status are compared, only the precision of Status 3 is lower than 90%.

**B. CONDITION IDENTIFICATION BY RF**

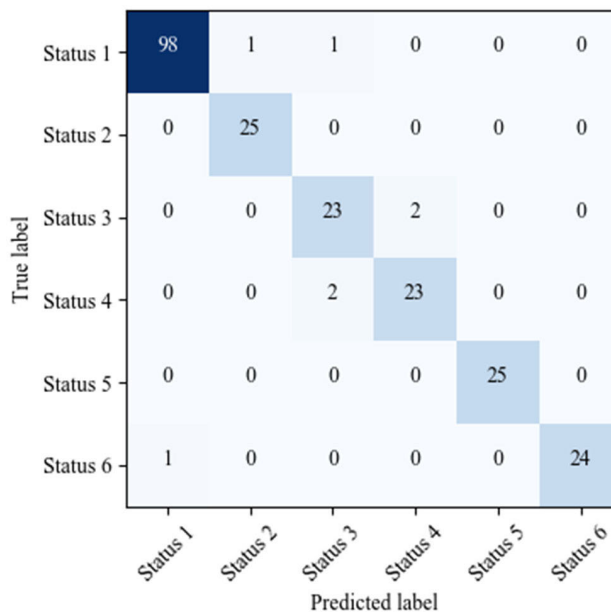
RF can be used to process high-dimensional and large-capacity data. Besides, the advantages of RF are: (1) not easy to over-fitting; (2) strong generalization performance; (3) suitable for small sample; (4) strong robust [25].

As the numbers of classifiers and features play important roles in RF, the values should be defined before the training process. The determination of the number of classifiers requires the following steps: first, the data set is divided into 5 mutually exclusive subsets of similar size and consistent data distribution by cross-validation; second, one of the subsets is selected as the test set, and the other 4 subsets are considered as the training set, and then the verification test is performed; third, 5 times of the verification tests are looped to ensure that each subset can be used as a test set; based on the above method, cross-validation scored the highest when the number of classifiers is selected as 60. Meanwhile, the features in RF are the same as those used in SVM.

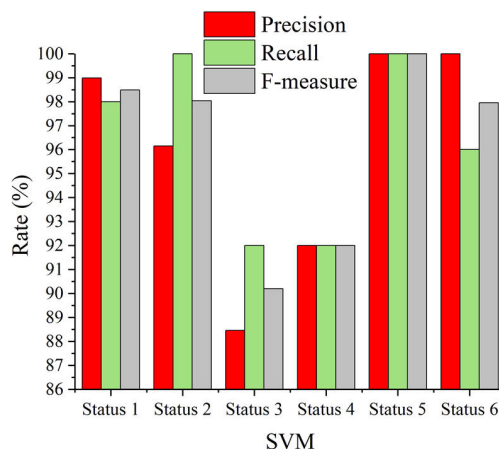
The diagnosis results of RF can be seen in FIGURE.8. Based on the confusion matrix, 3 sets of the testing data are not correctly identified. The precision, recall rate, and F-measure of each status are higher than 96%.

**C. CONDITION IDENTIFICATION BY DNN**

DNN is a deep learning algorithm based on neural networks and can be used as an unsupervised classifier. By the location of different layers in the DNN, the neural network layers can be divided into the input layer, the hidden layer,



a Confusion matrix



b Precision, recall rate, and F-measure for different status

FIGURE 7. Diagnosis results of SVM.

and the output layer. And, as the number of hidden layers of the network increases, the calculation process becomes more complicated. In other words, the more hidden layers, the longer the training times. The number of hidden layers is set to 5 after balancing the number of layers and the training time in the manuscript.

In the training process of DNN, the unsupervised learning process rate and the supervised learning rate are both set to 1, and the activation function is selected the Sigmoid function. The dimension of DNN features cannot be too many, so only closing time, maximum speed, closing speed, average speed, and overtravel are selected as the features.

The diagnosis results of DNN can be seen in FIGURE.9. Based on the confusion matrix, 20 sets of the testing data are not correctly identified. The precision, recall rate, and F-measure of Status 2 are all lower than 84%.

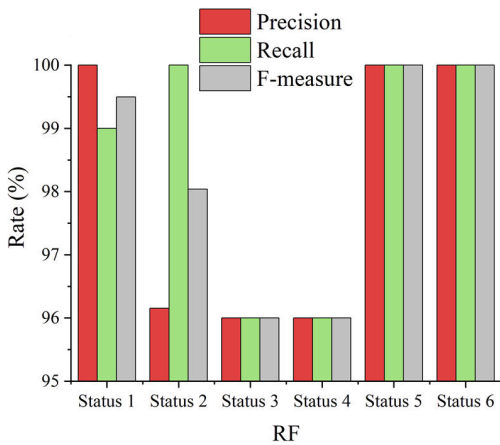
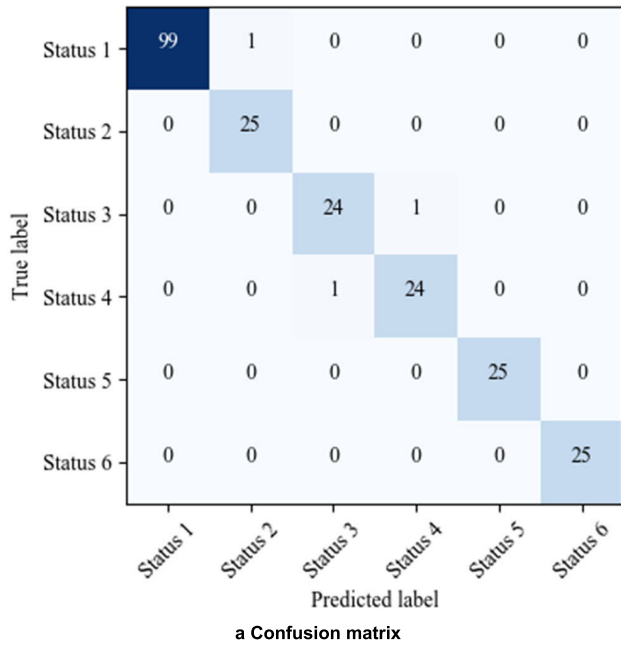


FIGURE 8. Diagnosis results of RF.

D. COMPARISON OF THE PERFORMANCE

The performances of the SVM, RF, and DNN in the condition identifying of the circuit breaker are compared, and the comparison results can be seen in TABLE 4. Combined with the precision, the recall rate, and the F-measure of each status, the inference can be drawn: the training time of RF is much smaller than SVM and DNN; the identification time of DNN is much longer than SVM and DNN; RF has the highest identifying accuracy. Generally, RF has the best diagnostic performance in the present paper.

TABLE 4. The comparison of different algorithms.

| Algorithm            | SVM   | RF    | DNN   |
|----------------------|-------|-------|-------|
| Features dimension   | 1003  | 1003  | 5     |
| Training time (s)    | 20.85 | 0.28  | 38.62 |
| Identifying time (s) | 0.007 | 0.008 | 2.35  |

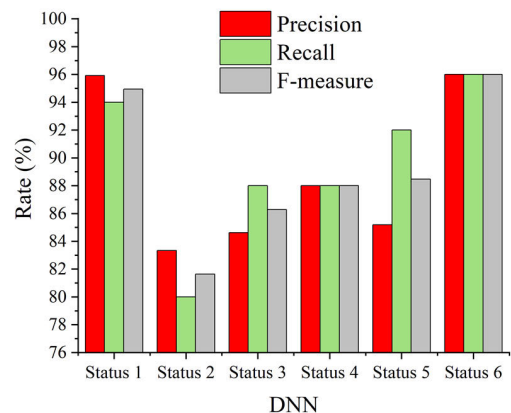
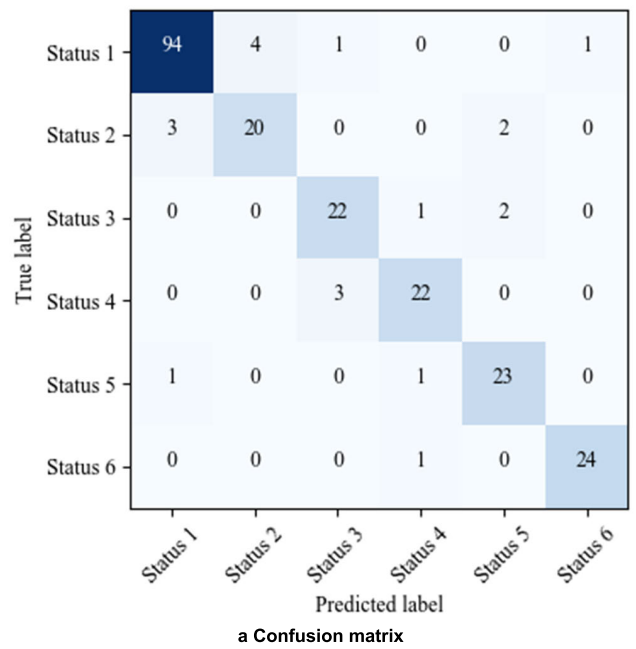


FIGURE 9. Diagnosis results of DNN.

V. LIFE PREDICTION

When the spring operation mechanism works, stress relaxation and fatigue are the most common failure modes, which will decrease the mechanical performances of the spring. As a result, the remaining useful life prediction of the spring is a valuable research issue. In the present section, the life models of spring under stress relaxation tests and life-cycle tests are established.

A. LIFE MODEL OF STRESS RELAXATION

The stress relaxation of spring can be described by a logarithmic equation,

$$\Delta P = (A + B \ln t_R) P_0 \tag{7}$$

where  $\Delta P$  is the increment of spring force,  $P_0$  is the initial spring force,  $A$  and  $B$  are dimensionless coefficients,  $t_R$  is time.

According to the above formula, the experimental data curve from FIGURE. 1 is subjected to regression processing, and the constants A and B in the second stage can be determined to be 0.0304 and 0.0154 respectively.

Based on the fitting model, the stress relaxation prediction model of the spring can be established. The spring used in the stress relaxation test is the same as the closing spring in the circuit breaker. Therefore, the influence of stress relaxation on closing speed can be calculated by the dynamic simulation model, which can be seen in FIGURE. 10.

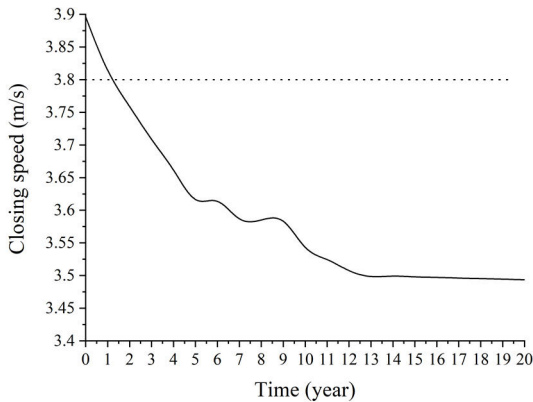


**FIGURE 10.** The relationship between closing speed and stress relaxation time.

The results indicate that the closing speed will lower than the rated closing speed after 1 year. From the results, the stress relaxation of the closing spring has a greater impact on the closing speed. However, the above defect only occurs in the energy-storing stage of the closing spring, and the stage lasts for a short time during the life cycle of the circuit breaker. As for the fatigue test, the speed drops fast after 5,500 times. Therefore, the traditional stress relaxation formula is not suitable for the circuit breaker under thousands of close-open operation tests, and a remaining useful life (RUL) model of the breaker is proposed based on the Wiener process.

**B. LIFE MODEL AT LIFE-CYCLE TEST**

Since Wiener Process can describe a non-monotonic performance degradation process, it has been widely used in the prediction of remaining useful life (RUL) [26], [27], such as lithium battery [28], turbofan engine [29], cutting tool [30], and brushless DC motor [31]. The predicted of RUL is more accurate by using the historical degradation information to estimate model parameters. The reason is that the degradation model established by using the prior information maintains the integrity of product degradation information, and the degradation trajectory of the same batch of products is similar under the same test conditions.

If a random process  $\{X(t), t \geq 0\}$  satisfies the following three conditions:

- 1)  $X(0) = 0$ ;
- 2)  $X(t)$  is a smooth independent incremental process;
- 3) when  $t > 0, X(s + t) - X(s) \sim N(0, \sigma^2 t)$ .

Then  $\{X(t), t \geq 0\}$  is named as the Wiener process, and it can be described as,

$$x(t) = \eta t + \sigma B(t) \tag{8}$$

where  $\eta$  is the drift coefficient reflecting individual degradation rate,  $t$  is time,  $\sigma$  is the diffusion coefficient,  $B(t)$  is standard Brownian motion.

The opening speed is more worthy of attention compared with closing speed, because once the circuit breaker cannot extinguish the electric arc and fails to break the fault current when the opening speed is not fast enough, which will lead to a large scale blackout and make great economic losses. Furthermore, the opening speed is influenced by opening spring, and the closing speed is influenced by both closing and opening spring, that is, the influence parameters of opening speed are less than that of closing speed.

Moreover, unlike traditional methods, the present paper defines the number of remaining operations as the index of the RUL, instead of the remaining time.

Based on the above, the degradation values of opening speed are used to predict the RUL of the circuit breaker by the Wiener Process. The degradation can be calculated as,

$$\Delta v = v_0 - v_t \tag{9}$$

where  $v_0$  is the initial value of speed,  $v_t$  is the speed at  $t$  time,  $\Delta v$  is the degradation value.

Based on the least squares estimation of  $\eta$  and  $\sigma$ , the prediction model is established. The fitting curve can be seen in FIGURE. 11, while, the fitting parameters can be seen in TABLE 5.

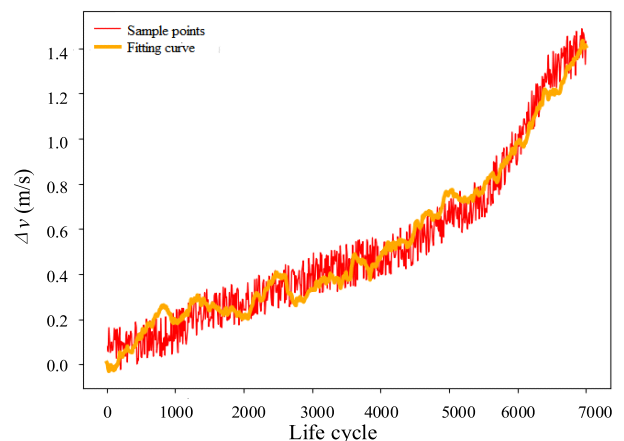


**FIGURE 11.** Life prediction of the operation mechanism.

**TABLE 5.** The fitting parameters of wiener process.

| Parameter | $\eta$                | $\sigma$              | $R^2$ |
|-----------|-----------------------|-----------------------|-------|
| Value     | $1.95 \times 10^{-4}$ | $3.51 \times 10^{-3}$ | 0.95  |

From the Wiener fitting results, the opening speed can be accurately predicted by the prediction model, and then the prediction of RUL of the circuit breaker is realized. Compared



with the stress relaxation predicting model, the results indicate that stress relaxation has little influence on the breaking capacity of the breaker compared with metal fatigue. Therefore, only metal fatigue is considered in the mechanical condition identification. What's more, the normal state also takes into account the wear and degradation of the spring mechanism.

To verify the accuracy of the RUL model, an additional 10 sets of degradation data are obtained from the same circuit breaker and used to predict the opening speed. Then the comparative results between the actual measured values and the predicted values can be seen in TABLE 6.

**TABLE 6. Comparative results between measured and predicted values.**

| Life cycle | Predicted values (m/s) | Measured values (m/s) | Error between predicted and measured value (%) |
|------------|------------------------|-----------------------|--|
| 1000       | 8.7015                 | 8.7858                | 0.96   |
| 1500       | 8.3040                 | 8.7008                | 4.56   |
| 2000       | 8.5065                 | 8.6596                | 1.77   |
| 2500       | 8.4090                 | 8.5472                | 1.62   |
| 3000       | 8.3115                 | 8.4591                | 1.74   |
| 3500       | 8.2140                 | 8.3688                | 1.85   |
| 4000       | 8.1165                 | 8.3998                | 3.37   |
| 4500       | 8.0190                 | 8.3813                | 4.32   |
| 5000       | 7.9215                 | 8.1774                | 3.13   |
| 5500       | 7.8240                 | 8.1526                | 4.03   |

The errors between predicted and measured values are all less than 5%, as a result, the RUL of the spring operating mechanism can be accurately described by Wiener Process.

## VI. DISCUSSIONS

The analysis of most previous works indicates the contact displacement, the coil current, and the vibration characteristics are mostly used in the diagnosis of the circuit breaker. However, some installation methods of the vibration sensors may damage the mechanical structure, and the installation positions will affect the diagnosis results. Due to the diversity of operating mechanisms, the installation positions of vibration sensors of different types of circuit breakers are quite different. The coil current can reflect circuit faults such as coil voltage, which is inconsistent with the types of fault simulated in the present paper. The contact displacement signal is obtained from the displacement sensor that is installed on the insulated pull rod. Compared with the vibration signal, the contact displacement signal has the great advantages of being less affected by the installation position of the circuit breaker, the fixing method of the sensor, and the load voltage level. Therefore, the contact displacement

is used to construct a feature matrix in the diagnosis and to predict the remaining breaking times of the circuit breaker.

In the stress relaxation test, the stiffness coefficient drops fast in the first 6 months, then descends very slowly. By fitting the relaxation model, the minimum rated opening speed is hardly reached even in long-term operation. However, the situation in the life-cycle test is different. With the increase of operation times, the opening speeds drop fast, especially after 6,000 times. Therefore, in the operation of the circuit breaker, it is important to consider the influence of the number of breaking times on the mechanical performance of the spring operation mechanism.

## VII. CONCLUSION

By spring stress relaxation test, life-cycle test, failure simulated test, and combined with the simulation model, the methods of identification and prediction of the spring operation mechanism are discussed in the present paper. The conclusions are as follows:

- 1) In the spring stress relaxation test, the stiffness coefficient of the spring will drop quickly in the first 6 months, then the downward trend slowed down.
- 2) The normal state, closing spring fatigue, opening spring fatigue, leak of oil buffer, and compound failures are all identified by SVM, RF, and DNN. The comparison results show that the conditions of the circuit breaker are identified by RF in the shortest time and most accurately.
- 3) In the frequent operation of the circuit breaker, the fitting curve from the stress relaxation test is not suitable, and the RUL of the spring operation mechanism can be accurately predicted by the Wiener process.
- 4) Comparing the metal fatigue life and stress relaxation life of the spring operating mechanism, the results indicate that the breaking times should be paid more attention than the operation time.

## REFERENCES

- [1] W. H. Niu, G. S. Liang, H. J. Yuan, and B. S. Li, "A fault diagnosis method of high voltage circuit breaker based on moving contact motion trajectory and ELM," *Math. Problems Eng.*, vol. 2016, p. 10, Jan. 2016.
- [2] B. Stephen, S. M. Strachan, S. D. J. McArthur, J. R. McDonald, and K. Hamilton, "Design of trip current monitoring system for circuit breaker condition assessment," *IET Gener., Transmiss. Distrib.*, vol. 1, no. 1, pp. 89–95, Jan. 2007.
- [3] T. Ji, L. Yi, W. Tang, M. Shi, Q. Wu, "Multi-mapping fault diagnosis of high voltage circuit breaker based on mathematical morphology and wavelet entropy," *CSEE J. Power Energy Syst.*, vol. 5, no. 1, pp. 130–138, 2019.
- [4] S. L. Ma, M. X. Chen, J. W. Wu, Y. H. Wang, B. W. Jia, and Y. Jiang, "Intelligent fault diagnosis of HVCB with feature space optimization-based random forest," *Sensors*, vol. 18, no. 4, p. 20, Apr. 2018.
- [5] S. Wan, L. Dou, C. Li, P. Wu, and R. Liu, "Study on on-line detection of characteristic parameters in high voltage circuit breaker opening process based on vibration signal," *Electr. Power Compon. Syst.*, vol. 46, no. 18, pp. 1969–1978, Nov. 2018.
- [6] A. A. Razi-Kazemi, K. Niayesh, and R. Nilchi, "A probabilistic model-aided failure prediction approach for spring-type operating mechanism of high-voltage circuit breakers," *IEEE Trans. Power Del.*, vol. 34, no. 4, pp. 1280–1290, Aug. 2019.

- [7] T. Li, Q. Zhou, L. Liu, S. Lin, and Z. Mou, "High-voltage circuit breaker fault diagnosis model based on coil current and KNN," in *Proc. Syst. Health Manage. Conf. (PHM-Chongqing)*, Chongqing, China, Oct. 2018, pp. 405–409.
- [8] Y. Pan, F. Mei, H. Miao, J. Zheng, K. Zhu, and H. Sha, "An approach for HVCB mechanical fault diagnosis based on a deep belief network and a transfer learning strategy," *J. Electr. Eng. Technol.*, vol. 14, no. 1, pp. 407–419, Jan. 2019.
- [9] S. S. Biswas, A. K. Srivastava, and D. Whitehead, "A real-time data-driven algorithm for health diagnosis and prognosis of a circuit breaker trip assembly," *IEEE Trans. Ind. Electron.*, vol. 62, no. 6, pp. 3822–3831, Jun. 2015.
- [10] A. A. Razi-Kazemi, "Circuit breaker condition assessment through a fuzzy-probabilistic analysis of actuating coil's current," *IET Gener., Transmiss. Distrib.*, vol. 10, no. 1, pp. 48–56, Jan. 2016.
- [11] Q. Yang, J. Ruan, Z. Zhuang, D. Huang, and Z. Qiu, "A new vibration analysis approach for detecting mechanical anomalies on power circuit breakers," *IEEE Access*, vol. 7, pp. 14070–14080, 2019.
- [12] S. Ma, M. Chen, J. Wu, Y. Wang, B. Jia, and Y. Jiang, "High-voltage circuit breaker fault diagnosis using a hybrid feature transformation approach based on random forest and stacked autoencoder," *IEEE Trans. Ind. Electron.*, vol. 66, no. 12, pp. 9777–9788, Dec. 2019.
- [13] N. T. Huang, H. J. Chen, G. W. Cai, L. H. Fang, and Y. Q. Wang, "Mechanical fault diagnosis of high voltage circuit breakers based on variational mode decomposition and multi-layer classifier," *Sensors*, vol. 16, no. 11, p. 19, Nov. 2016.
- [14] F. N. Rudsari, A. A. Razi-Kazemi, and M. A. Shoorehdeli, "Fault analysis of high-voltage circuit breakers based on coil current and contact travel waveforms through modified SVM classifier," *IEEE Trans. Power Del.*, vol. 34, no. 4, pp. 1608–1618, Aug. 2019.
- [15] A. Janssen, D. Makareinis, and C.-E. Solver, "International surveys on circuit-breaker reliability data for substation and system studies," *IEEE Trans. Power Del.*, vol. 29, no. 2, pp. 808–814, Apr. 2014.
- [16] C. Feng, Y. Xie, J. Wang, D. Li, W. Chen, W. Li, and K. Ouyang, "Study on typical metal fatigue failure of circuit breaker operating mechanism unit," *IOP Conf. Mater. Sci. Eng.*, vol. 392, Aug. 2018, Art. no. 022026.
- [17] M. Fangang, W. Shijing, H. Jicai, X. Yang, J. Junfeng, L. Qiaoquan, and S. Cunling, "Simulation and stability analysis of spring operating mechanism with clearance for high voltage circuit breakers," in *Proc. China Int. Conf. Electr. Distrib. (CICED)*, Xi'an, China, Aug. 2016, pp. 1–5.
- [18] C. X. Ren, D. Q. Q. Wang, Q. Wang, Y. S. Guo, Z. J. Zhang, C. W. Shao, H. J. Yang, and Z. F. Zhang, "Enhanced bending fatigue resistance of a 50CrMnMoVNb spring steel with decarburized layer by surface spinning strengthening," *Int. J. Fatigue*, vol. 124, pp. 277–287, Jul. 2019.
- [19] D. Pastorcic, G. Vukelic, and Z. Bozic, "Coil spring failure and fatigue analysis," *Eng. Failure Anal.*, vol. 99, pp. 310–318, May 2019.
- [20] H. Huang, F. Wang, Y. Lu, X. Xia, and Y. Su, "A new test method of circuit breaker spring telescopic characteristics based image processing," in *Proc. E3S Web Conf.*, vol. 38, 2018, p. 04022.
- [21] A. R. R. Matavalam and A. K. Bharati, "Reliability assessment of industrial circuit breakers with design enhancements," in *Proc. IEEE Int. Conf. Probabilistic Methods Appl. Power Syst. (PMAPS)*, Boise, ID, USA, Jun. 2018, pp. 1–6.
- [22] T. M. Lindquist, L. Bertling, and R. Eriksson, "Circuit breaker failure data and reliability modelling," *IET Gener., Transmiss. Distrib.*, vol. 2, no. 6, pp. 813–820, Nov. 2008.
- [23] M. Abbasghorbani and H. R. Mashhadi, "Circuit breakers maintenance planning for composite power systems," *IET Gener., Transmiss. Distrib.*, vol. 7, no. 10, pp. 1135–1143, Oct. 2013.
- [24] H. Shao, H. Jiang, H. Zhang, W. Duan, T. Liang, and S. Wu, "Rolling bearing fault feature learning using improved convolutional deep belief network with compressed sensing," *Mech. Syst. Signal Process.*, vol. 100, pp. 743–765, Feb. 2018.
- [25] L. Breiman, "Random forests," *Mach. Learn.*, vol. 45, no. 1, pp. 5–32, 2001.
- [26] X. Wang, C. Hu, X. Si, Z. Pang, and Z. Ren, "An adaptive remaining useful life estimation approach for newly developed system based on nonlinear degradation model," *IEEE Access*, vol. 7, pp. 82162–82173, 2019.
- [27] Y. Lyu, Y. Zhang, K. Chen, C. Chen, and X. Zeng, "Optimal multi-objective burn-in policy based on time-transformed Wiener degradation process," *IEEE Access*, vol. 7, pp. 73529–73539, 2019.
- [28] Z. Zhang, D. X. Shen, Z. Peng, Y. Guan, H. M. Yuan, and L. F. Wu, "Lithium-ion batteries remaining useful life prediction method considering recovery phenomenon," *Int. J. Electrochem. Sci.*, vol. 14, no. 8, pp. 7149–7165, Aug. 2019.
- [29] N. Li, Y. Lei, T. Yan, N. Li, and T. Han, "A wiener-process-model-based method for remaining useful life prediction considering unit-to-unit variability," *IEEE Trans. Ind. Electron.*, vol. 66, no. 3, pp. 2092–2101, Mar. 2019.
- [30] H. Sun, D. Cao, Z. Zhao, and X. Kang, "A hybrid approach to cutting tool remaining useful life prediction based on the Wiener process," *IEEE Trans. Rel.*, vol. 67, no. 3, pp. 1294–1303, Sep. 2018.
- [31] Q. Yuan, J. Ye, and X. Li, "Multistage temperature degradation modeling for BLDC motor based on Wiener process," *J. Beijing Univ. Aeronaut. Astronaut.*, vol. 44, no. 7, pp. 1514–1519, Jul. 2018.



**YAKUI LIU** was born in Shandong, China, in 1990. He received the B.S. degree from Linyi University, Shandong, China, in 2013, and the M.S. degree from the Qilu University of Technology, Shandong, China, in 2016. He is currently pursuing the Ph.D. degree with the State Key Laboratory of Electrical Insulation and Power Equipment, Xi'an Jiaotong University, Xi'an, China.

His current research interests include electrical contact theory and intelligent electrical apparatus.



**GUOGANG ZHANG** (Member, IEEE) was born in Shaanxi, China, in 1976. He received the Ph.D. degrees from Xi'an Jiaotong University, Xi'an, China, in 2004. He is currently a Professor with the State Key Laboratory of Electrical Insulation and Power Equipment, Xi'an Jiaotong University.

His current research interests include theory and application of intelligent electrical apparatus, electric arc plasma and electrical contact theory, and power equipment for renewable energy. He is a Committee Member of the Low Voltage Electrical Apparatus Committee of the China Electrotechnical Society.



**CHENCHEN ZHAO** was born in Shaanxi, China, in 1998. She received the bachelor's degree from the Xi'an University of Technology, Xi'an, China, in 2019. She is currently pursuing the master's degree with the State Key Laboratory of Electrical Insulation and Power Equipment, Xi'an Jiaotong University. Her current research field is the theory and application of smart appliances.



**SHENG LEI** was born in Shaanxi, China, in 1996. He received the bachelor's degree from the Xi'an University of Technology, Xi'an, China, in 2019. He is currently pursuing the master's degree with the State Key Laboratory of Electrical Insulation and Power Equipment, Xi'an Jiaotong University. His research field is intelligent electrical fault diagnosis.



**HAO QIN** was born in Shaanxi, China, in 1994. He received the bachelor's degree from Xi'an Jiaotong University, in 2017, where he is currently a graduate student with the State Key Laboratory of Electrical Insulation and Power Equipment. His current research field is the theory and application of smart appliances.



**JINGGANG YANG** (Member, IEEE) was born in Shaanxi, China, in 1984. He received the M.S. degree from Xi'an Jiaotong University, Xi'an, China, in 2009.

He is currently with the Jiangsu Electric Power Company Research Institute, State Grid Corporation of China. His current research interests include electrical contact theory and intelligent electrical apparatus.

...